(NASA-CR-164292) COMPRESSIBLE TURBULENT BOUNDARY LAYER INTERACTION EXPERIMENTS Final Technical Report, 1 Feb. 1978 - 31 Jan. 1981 (Princeton Univ., N. J.) 37 p HC A03/MF A01 CSCL 20D G3/34

N81-23415

Unclas 42307

Princeton University

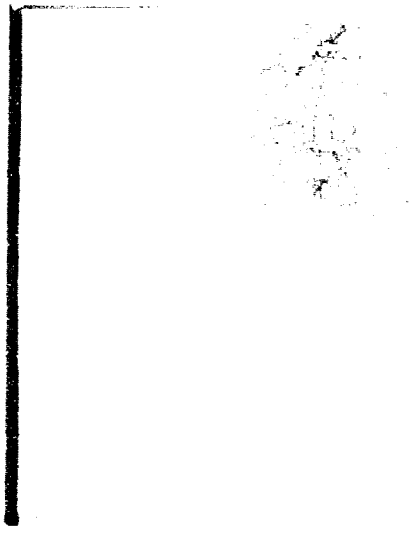

Department of
Mechanical and
Aerospace Engineering

MAE REPORT 1525

COMPRESSIBLE TURBULENT BOUNDARY LAYER INTERACTION EXPERIMENTS

by

Gary S. Settles

FINAL TECHNICAL REPORT
FOR THE PERIOD
FEBRUARY 1, 1978 TO JANUARY 31, 1981

NASA GRANT NSG-2299

PRINCETON UNIVERSITY
Department of Mechanical & Aerospace Engineering
Gas Dynamics Laboratory
Forrestal Campus
Princeton, NJ 08544

May 1981

TABLE OF CONTENTS

INTRODUCTION

This Final Technical Report summarizes research results obtained by the Gas Dynamics Laboratory, Mechanical and Aerospace Engineering Department, Princeton University, under NASA Grant NSG-2299. This Grant, entitled "Compressible Turbulent Boundary Layer Interaction Experiments," extended from February 1, 1978 to January 31, 1981. The Co-Principal investigators of the research study were Dr. Gary S. Settles and Prof. Seymour M. Bogdonoff. Dr. C. C. Horstman of NASA Ames Research Center served as NASA Technical Officer and was also significantly involved in part of the research effort on a cooperative basis. Some of the studies reported here were jointly supported by the USAF Office of Scientific Research under Contracts F44620-75-C-0080 and F49620-80-C-0092.

In the following summary, four phases of research results are reported: 1) experiments on the compressible turbulent boundary layer flow in a streamwise corner, 2) the two-dimensional (2D) interaction of incident shock waves with a compressible turbulent boundary layer, 3) three-dimensional (3D) shock/boundary layer interactions, and 4) cooperative experiments at Princeton and numerical computations at NASA-Ames. Since much of this work has either appeared in the open literature or been reported previously to NASA (see REFERENCES and PUBLICATIONS BIBLIOGRAPHY), the present account is appropriately abbreviated.

I. A STREAMWISE CORNER IN COMPRESSIBLE TURBULENT FLOW

1. Introduction

The joining of two boundary layers at a streamwise corner is an important problem in aerodynamic design and in the basic understanding of complex flows. Beginning with Carrier[1], several investigators[2-5] have analyzed the problem for laminar flow, thus avoiding the obvious intractability of turbulent motion. Fluid compressibility was, however, taken into account in the analyses of Refs. 3 and 4. These investigators agree that an important feature of the streamwise corner is an imbedded secondary flow consisting of counter-rotating vortices. For the laminar case, the direction of the secondary flow along the corner bisector is found to be outward, away from the corner.

Both theoretical and experimental results are available for the incompressible turbulent streamwise corner flow (e.g., Refs. 6-8), in which an inward motion is detected along the corner bisector. The detailed measurements by Gessner[7], Mojola and Young[8], and others, show that the three-dimensional and turbulent aspects of this flow are intimately related.

For the case of the streamwise corner in compressible turbulent flow, a number of experiments[9-11] and at least one numerical computation[12] are available. In these studies, intersecting plates or wedges were used to generate the corner flow, leading to a strong interaction between the turbulent boundary layer and the shock waves originating from the wedge leading edges. Under such conditions the corner flow is dominated by a complex imbedded shock wave system which precludes the study of the comparatively weak secondary flow contributions due to the turbulence itself in such experimental geometries.

In contrast to the above, an unbounded streamwise corner flow offers a certain elegance of simplicity; it is turbulent, compressible, and fully three-dimensional, but has no shock wave system or streamwise pressure gradient. This note describes an experimental attempt to study such an unbounded corner in a supersonic channel flow, as diagrammed in Fig. 1.

2. Experimental Arrangement

The streamwise corner flow of this study is that which develops in the 20.3 cm. square channel downstream of the nozzle of the Princeton High Reynolds Number Wind Tunnel. The test conditions include a Mach number of 2.9, a freestream Reynolds number of 6.3×10^7/meter, a stagnation pressure of 0.69 MN/m^2, and an approximately adiabatic wall. The corner region was surveyed with a 7-tube pitot rake which traversed normal to both the channel floor and sidewall. These rake surveys were carried out in sections 1 and 2 of the channel, at distances of 0.28 and 1.18 meters from the nozzle exit, respectively. Measurements were also taken of surface pressures and streak lines.

3. Results and Discussion

Figures 2 and 3 display the lines of constant pitot pressure in the corner region at the two streamwise test stations. For both stations, the region of corner influence is confined to 2 or 3 cm. from the corner location. The floor boundary layer approaching the corner is quite uniform in the Z direction. (This boundary layer has been extensively surveyed at Z = 10 cm. and was found to be in an equilibrium state.) Such is not the case for the adjoining sidewall boundary layer, which is thinner than the floor boundary layer near the corner, and which grows significantly in thickness as Y increases. Thus, the corner flow is not symmetric about a bisector at either streamwise test station.

The reason for this asymmetry lies in the inviscid wave system generated in the two-dimensional wind tunnel nozzle. As illustrated in Fig. 1, the static pressure at the sidewall center inside the nozzle is lower than that at the corners (an effect that is not present on the nozzle floor or ceiling). Thus a secondary flow is induced, which causes boundary layer fluid to "pile up" along the sidewall centerlines. This effect has been known since the early days of supersonic wind tunnel testing.[13,14] How seriously it affects the corner flow symmetry can be judged from Figs. 2 and 3. The sidewall "bumps" appear to grow with increasing X, and will eventually join together far downstream. Also, this effect is expected to grow worse at higher nozzle exit Mach numbers, which seems to be confirmed by measurements reported in Ref. 15. Sublayer fences on the nozzle sidewall have been used[14] to partially alleviate this secondary flow by breaking up the nozzle pressure gradient.

The sidewall static pressure distribution was measured at both test stations and found to be constant and equal to the freestream static pressure within $\pm 1\%$. This fact makes it reasonable to assume that the entire corner flow exists at a constant static pressure. In such a case, the pitot isobars of Figs. 2 and 3 are equivalent to lines of constant velocity. The velocity profiles thus obtained have been analyzed using a compressible "Clauser plot" technique to yield the estimates of skin friction coefficient shown in Fig. 4.

The c_f values on the channel floor in Fig. 4 are roughly constant at about the values given by the Van Driest II theory. In contrast, c_f on the sidewall increases toward the corner, reflecting the relative thinning of the adjoining boundary layer there.

The measured surface streak lines show a very slight divergence away from the corner. This divergence does not clearly indicate anything more than the growth of boundary layer displacement thickness in the corner region with increasing X.

II. 2D INCIDENT SHOCK/BOUNDARY LAYER INTERACTIONS

1. Introduction

This study of the incident shock wave/turbulent boundary layer interaction was intended to supplement previous work[16-21] and to provide critical data for the mathematical modeling of turbulent flows. In particular, the effects of streamwise curvature were to be assessed by comparing the incident-shock interaction with the data from compression corner experiments[22] at the same flow conditions. As there has always been some doubt about the two-dimensionality of the flow in the previous incident-shock studies, we first concentrated on examining this important aspect of the flowfield.

The experiment was carried out in the Princeton University 20 x 20 cm. Supersonic Wind Tunnel. The incident-shock wave generator, shown in Fig. 5, is 32.4 cm. long and 19.7 cm. wide, and is not sealed at the sidewalls. The shock generator angle, α, can be continuously varied around a pivot located at a front part of the shock generator, as illustrated in Fig. 5. The generator angles tested were 4°, 8° and 10°. The pressure behind the generated shock wave was measured by an orifice located 12.7 cm. from the leading edge of the shock generator on its centerline. The angle of the shock generator was set by reading this pressure during the run, considering the influence of the boundary layer displacement thickness to

the apparent angle of the shock generator, and adjusting the generator angle accordingly.

The test conditions were: Mach number = 2.95, stagnation pressure = 6.80 atm, stagnation temperature = 258°K ± 5%, and free stream unit Reynolds number = 6.10×10^7/meter. The incoming turbulent boundary layer had an overall thickness, δ_o , of about 1.5 cm.

In order to check the two-dimensionality of the interaction, surface oil flow techniques, surface static pressure measurements, and pitot pressure surveys were carried out. Aerodynamic fences were used to prevent secondary flow from the sidewalls. The geometries of the two fence configurations are shown in Fig. 6, and a table of fence configurations for the test series is given. Note that "double fences" (configuration B) were used in one case in an attempt to properly isolate the interaction region.

2. Results

Surface Flow Patterns

Surface oil flow patterns for $\alpha = 8°$ and $\alpha = 10°$ are shown in Figs. 7-11. Without aerodynamic fences, strong three-dimensional disturbances are observed after boundary layer separation (denoted by "S"). The reattachment line is quite curved compared to the separation line. For $\alpha = 8°$, the separation line appears reasonably straight even without fences, but a strong inflow from the sidewalls is observed near the separated region. With a change of fence position, the shape and location of the separation line also changes slightly, while the reattachment line is always curved and the three-dimensionality is not eliminated.

Surface Pressure Distributions

Shown in Fig. 12 are the streamwise surface pressure distributions for $\alpha = 8°$ and 10°, measured along the centerline. The upstream influence

starts about 1.7 δ_0 for α = 8° and 2.2 δ_0 for α = 10°. The separation and reattachment locations are denoted in Fig. 12 by "S" and "R". The pressure level after the interaction is lower than the theoretical inviscid level, which is shown by dotted lines in Fig. 12. Further, the measured pressure distributions exhibit a "peak" followed by a slight pressure decrease. This pressure decrease seems to be due to the strong three-dimensionality of the flow after reattachment. It is noticed from the surface patterns that there is a secondary flow inward from the fences toward the centerline at the beginning of interaction, followed by an outward flow from the centerline toward the fences further downstream. This outward flow seems to correspond to the pressure decrease after the "peak". This pressure decrease becomes smaller as the fence distance, W, decreases, as shown in Fig. 13.

As a further indication of the spanwise uniformity of the flow, spanwise pressure distributions are shown for α = 8° at several test stations in Fig. 14. One notes in this figure that the initial flow just upstream of the interaction is quite uniform in the spanwise direction. However, as one progresses downstream through the interaction, symmetrical variations occur in the spanwise pressures. At first, these distributions become "cupped" so that a maximum pressure is seen near the tunnel centerline. Further downstream this trend reverses, the centerline pressure dropping below that at the sides. These measurements clearly indicate the progressively three-dimensional secondary flow phenomena which appear under the influence of the incident shock wave.

Pitot Pressure Measurements

Pitot surveys were carried out to determine if the incoming shock wave was planar. The pitot pressures just ahead of and behind the shock

were measured in the crosswise direction using a streamlined probe. The survey height was about 6.4 cm, which is well ahead of the interaction with the floor boundary layer. We found some indications that the shock may already be slightly convex before the interaction begins.

3. Summary of Observations

After several attempts to create a two-dimensional flow field, the following observations are made:

a) The flow reattachment line shows a strong three-dimensionality. Just after reattachment the surface flow directs toward the centerline and then changes to an outward direction.

b) Aerodynamic fences seem to improve the flow ahead of the separation line, but not the flow after reattachment nor the reattachment line itself.

c) The region where the crosswise surface pressure distribution is uniform is only 5 cm. wide around the tunnel centerline. The aspect ratio of the separated region is about 4, which is too small to be considered as two-dimensional.

d) The pressure level after the interaction is generally lower than inviscid pressure level. There is also a slight decrease in pressure, apparently due to the three-dimensional flow after reattachment.

III. SCALING LAWS IN TWO- AND THREE-DIMENSIONAL SHOCK/BOUNDARY LAYER INTERACTIONS

1. A Brief Review of the State of the Art

Shock wave interactions with compressible turbulent boundary layers have been studied many times by past investigators. Most of these studies have concerned the two-dimensional or semi-infinite case because the investigators felt that the problem was already sufficiently complex without the

added difficulty of a third dimension. They proceeded to attempt to characterize these two-dimensional (2D) interactions through experimental measurements and some approximate calculations.

The earliest investigators (e.g., Refs. 23 and 24) learned that the streamwise length scales of these interactions depended upon Mach number, Reynolds number, overall pressure rise, incoming boundary layer thickness, and (sometimes) experimental geometry. Through the years, as a body of experimental evidence was built up, empirical correlations and approximate analyses have evolved into what we now know as the scaling laws of 2D shock/boundary layer interactions, which describe with reasonable accuracy the effects of the above parameters on interaction length scales.[25]

However, even with the simplifying assumption of 2D flow, some of these scaling laws have not been developed sufficiently to provide a general picture of the interaction scaling. For example, it has been commonly assumed[24,26] that the length scale of a 2D interaction is proportional to the incoming turbulent boundary layer thickness, δ_o , if all other parameters are held constant. Indeed, limited experimental data supported this view for many years. Only recently have more detailed studies[25,27,28] shown that this is an oversimplification, and that the unit Reynolds number is also an important part of the interaction scale.

Figure 15 (from Ref. 28) illustrates the Reynolds number and boundary layer thickness scaling of upstream influence ahead of Mach 3 compression corners, as we now understand it. Stated simply, if δ_o is taken as the interaction scale, then a Re_{δ_o} "residual" effect remains to be taken into account. This has been done in Fig. 15, where good agreement among the three leading experiments in the field is shown in terms of an empirical δ_o and Re_{δ_o} scaling function.

Still, the scaling of 2D interactions is not yet perfectly understood. The physical mechanism of upstream influence, for example, has been the subject of a long-term effort by many distinguished researchers, and is still not clear. Recent developments of the so-called "triple-deck theory"[29] may point the way to an eventual understanding of this mechanism (we hope).

So, while some questions remain about the generality and physical basis of the 2D interaction scaling laws, there is nevertheless a reasonable scaling framework with which to proceed. The situation for 3D interactions is, unfortunately, not nearly so good. Far fewer 3D experiments have been done, and each one has seemed to stand by itself with little obvious connection to the others. While the individual 3D experiments have shown some radical departures from the known 2D behavior, it has not been possible to judge from them how large a particular 3D interaction scale should be, or how it might vary with δ_0, Re, M_∞, shock strength, etc. Basic knowledge has been lacking, both in terms of a sufficient range of experimental measurements and a framework within which to relate them.

This problem has been studied in recent years by Settles, Dolling, Oskam, Bogdonoff, and other investigators at the Princeton University Gas Dynamics Laboratory. Our efforts have been concentrated on a particular class of simple 3D geometries which produce representative (though not necessarily simple) 3D interactions. This class of geometries, illustrated in Fig. 16, includes those which we call the "sharp fin," "swept fin," "blunt fin," and "swept compression corner."

In conducting experiments with this class of 3D interactions, our long-term goals are listed as follows:

1) develop scaling laws governing the individual interactions in terms of pertinent flow and geometric parameters,
2) develop a framework within which the scaling of the individual interactions can be related to the interaction class as a whole,
3) investigate, through detailed measurements, the physical mechanisms which occur within these interactions and give rise to their overall scaling behavior, and
4) provide detailed data sets, from these measurements, which can be used for code validation and turbulence model development in computational fluid dynamics.

We have made some progress in reaching each of the above goals so far, though much work remains to be done. For example, some basic scaling information on three of the four interactions of Fig. 16 is given in our recent publications.[28,30-33] One of the interactions — the sharp fin — has been surveyed extensively to yield detailed data which serves some of the purposes of goals 3 and 4 above.[30] Most recently, companion papers by Settles and Dolling[28,33] developed the Reynolds number and boundary layer thickness scaling laws for the swept corner and sharp fin, respectively, and showed how the two interactions are related in that sense (the general scaling law being the same for both).

Our most recent work is concentrating on the scaling behavior of the stated class of interactions in terms other than Reynolds number and boundary layer thickness, that is, shock strength, Mach number, sweepback angle, etc. This effort is expected to require both the further analysis of results already in hand and further experiments as well.

An important part of the experiments concerns the "swept fin" of Fig. 16, which is designed to generate a doubly-swept shock wave which skews across the incoming 2D turbulent boundary layer.

2. Swept Fin Interaction

Under NASA Grant NSG-2299 we conducted an exploratory set of experiments using the swept fin geometry. The geometry and range of parameters tested are shown in Fig. 17. So far, only surface flow visualization records have been taken for this set of experiments, as shown by an example kerosine-graphite trace in Fig. 18.

Briefly, these results showed that the swept fin interaction is more highly swept back than the corresponding unswept (sharp) fin interaction for equal values of the deflection angle α. Our immediate goal in these experiments was to compare the 3D interactions generated by the swept fin and the swept compression corner (ramp) under conditions of the same compound shock angle. As shown in Fig. 19, there is a region of overlap of these two interactions in terms of shock angle (thus also overall pressure rise) at Mach 3.

For the time being we have not been able to make this comparison, since it requires knowledge of the inviscid shock location in the swept fin case. Obtaining this information is an important part of our continuing research under new NASA sponsorship.

IV. COOPERATIVE EXPERIMENTS AND COMPUTATIONS

In the past, useful progress has been made in a cooperative effort of experiments by the present investigators and computational solutions of the time-averaged Navier-Stokes equations by Dr. C. C. Horstman of NASA-Ames. A good example of such cooperative efforts — carried out

under previous funding from NASA — is given in Ref. 34.

During the course of NASA Grant NSG-2299 this cooperative effort was continued. Specifically, the results of a flow reattachment experiment we conducted under other sponsorship were compared with a computational simulation of that flow, carried out by Dr. Horstman. With a large 2D separation zone, this particular experiment[35] is a particularly difficult one to compute. However, Dr. Horstman's solution was generally successful and revealed several interesting points which pace future progress. This cooperative effort was reported at a recent AIAA Meeting (see PUBLICATIONS BIBLIOGRAPHY).

The present investigators are also participating in the 1980-81 AFOSR-HTTM-Stanford Conference on Complex Turbulent Flows, at which a general effort is being made to identify "benchmark" experiments and to evaluate current solution methods. In fact, several of our past experiments were accepted for the Data Library of this Conference, including some work carried out under previous NASA support. Dr. Horstman of NASA, and others from various organizations, are now performing calculations to be compared with the experiments in the Data Library at the upcoming second meeting of the Stanford Conference (September 1981).

V. PUBLICATIONS BIBILIOGRAPHY

1) Settles, G. S. and Bogdonoff, S. M., Annual Status Report, NASA Grant NSG-2299, Feb. 1, 1978 to Jan. 31, 1979 (May 1979).

2) Settles, G. S. and Bogdonoff, S. M., Semi-Annual Status Report, NASA Grant NSG-2299, Feb. 1, 1979 to July 31, 1979 (August 1979).

3) Tsumuraya, M., "An Experimental Study of Incident Shock Wave/Turbulent Boundary Layer Interactions," M.S.E. Thesis, Mech. & Aerospace Engrg.

Dept., Princeton University, Dec. 1980.

4) Horstman, C. C., Settles, G. S., Williams, D. R., and Bogdonoff, S. M., "A Reattaching Free Shear Layer in Compressible Turbulent Flow - A Comparison of Numerical and Experimental Results," AIAA Paper 81-0333, presented at AIAA 19th Aerospace Sciences Mtg., St. Louis, Missouri, 12-15 January 1981.

REFERENCES

1) Carrier, G. F., "The Boundary Layer in a Corner," Quarterly of Applied Mathematics, Vol. 4, No. 4, 1947, pp. 367-378.

2) Moore, F. K., "Three-Dimensional Boundary Layer Theory," Advances in Applied Mechanics, Vol. IV, 1956, pp. 159-228.

3) Libby, P. A., "Secondary Flows Associated with a Supersonic Corner Region," AIAA Journal, Vol. 4, June 1966, pp. 1130-1132.

4) Weinberg, B. C. and S. G. Rubin, "Compressible Corner Flow," Journal of Fluid Mechanics, Vol. 56, Part 4, 1972, pp. 753-774.

5) Ghia, K. N., "Incompressible Streamwise Flow Along an Unbounded Corner," AIAA Journal, Vol. 13, July 1975, pp. 902-907.

6) Shafir, M. and S. G. Rubin, "The Turbulent Boundary Layer Near a Corner," Journal of Applied Mechanics, Vol. 98, Dec. 1976, pp. 567-570.

7) Gessner, F. B., "The Origin of Secondary Flow in Turbulent Flow Along a Corner," Journal of Fluid Mechanics, Vol. 58, Part 1, 1973, pp. 1-25.

8) Mojola, O. O. and A. D. Young, "An Experimental Investigation of the Turbulent Boundary Layer Along a Streamwise Corner," AGARD CP-93, 1972, Paper #12.

9) Charwat, A. F. and L. G. Redekopp, "Supersonic Interference Flow Along the Corner of Intersecting Wedges," AIAA Journal, Vol. 5, March 1967, pp. 480-488.

10) West, J. E. and R. H. Korkegi, "Supersonic Interaction in the Corner of Intersecting Wedges at High Reynolds Numbers," AIAA Journal, Vol. 10, May 1972, pp. 652-658.

11) Oskam, B., I. E. Vas and S. M. Bogdonoff, "An Experimental Study of Three-Dimensional Flow Fields in an Axial Corner at Mach 3," AIAA Paper 77-689, June 1977.

12) Shang, J. S., W. L. Hankey and J. S. Petty, "Three-Dimensional Interacting Turbulent Flow Along a Corner," AIAA Paper 78-1210, July 1978.

13) Bollay, W., "Aerodynamics of Supersonic Aircraft and Missiles," U. S. Navy Report NOLR 1131, June 1949, pp. 27-50.

14) Haefeli, R. C., "Use of Fences to Increase Uniformity of Boundary Layer on Side Walls of Supersonic Wind Tunnels," NACA RM E52E19, July 1952.

15) Kitchens, C. W., Jr., C. C. Bush and R. Sedney, "Characteristics of the Sidewall and Floor Boundary Layers in BRL Supersonic Wind Tunnel No.1," USA Ballistic Research Labs, BRL MR2563, Dec. 1975.

16) Bogdonoff, S. M., C. E. Kepler, and E. Sanlorenzo, "A Study of Shock Wave Turbulent Boundary Layer Interaction at M = 3," Princeton University Aeronautical Engineering Dept., Rpt. 222, July 1953.

17) Pinckney, S. Z., "Data on Effects of Incident-Reflecting Shocks on the Turbulent Boundary Layer," NASA TM X-1221, March 1966.

18) Green, J. E., "Reflection of an Oblique Shock Wave by a Turbulent Boundary Layer," J. Fluid Mech., Vol. 40, Part I, pp. 81-95, 1970.

19) Reda, D. C. and J. D. Murphy, "Shock Wave-Turbulent Boundary Layer Interactions in Rectangular Channels," AIAA Paper 72-715, June 1972.

20) Reda, D. C. and J. D. Murphy, "Shock Wave-Turbulent Boundary Layer Interactions in Rectangular Channels, Part II: The Influence of Sidewall Boundary Layers on Incipient Separation and Scale of the Interaction," AIAA Paper 73-234, January 1973.

21) Law, C. H., "Two-Dimensional Compression Corner and Planar Shock Wave Interactions with a Supersonic, Turbulent Boundary Layer," USAF ARL Rept. 0157, June 1975.

22) Settles, G. S., "An Experimental Study of Compressible Turbulent Boundary Layer Separation at High Reynolds Numbers," Ph.D. Dissertation,

Aerospace and Mechanical Sciences Dept., Princeton University, Princeton, NJ, September 1975.

23) Bogdonoff, S. M. and C. E. Kepler, "Separation of a Supersonic Turbulent Boundary Layer," J. Aero. Sci., 22, 1955, pp. 414-424.

24) Drougge, G., "Experimental Investigation of the Influence of Strong Adverse Pressure Gradients on Turbulent Boundary Layers at Supersonic Speeds," 6th Intn'l. Congress on Theoretical and Applied Mechanics, Istanbul, 1952.

25) Green, J. E., "Interactions Between Shock Waves and Boundary Layers," Progress in Aerospace Sciences, Vol. 11, 1970, pp. 235-340.

26) Erdos, J. and A. Pallone, "Shock-Boundary Layer Interaction and Flow Separation," AVCO RAD-TR-61-23, 1961.

27) Settles, G. S., S. M. Bogdonoff and I. E. Vas, "Incipient Separation of a Supersonic Turbulent Boundary Layer at High Reynolds Numbers," AIAA Journal, Vol. 14, Jan. 1976, pp. 50-56.

28) Settles, G. S., J. J. Perkins and S. M. Bogdonoff, "Upstream Influence Scaling of 2D and 3D Shock/Turbulent Boundary Layer Interactions at Compression Corners," AIAA Paper 81-0334, January 1981.

29) Inger, G. R., "Upstream Influence and Skin Friction in Non-Separating Shock-Turbulent Boundary Layer Interactions," AIAA Paper 80-1411, July 1980.

30) Oskam, B., I. E. Vas and S. M. Bogdonoff, "Mach 3 Oblique Shock Wave/Turbulent Boundary Layer Interactions in Three Dimensions," AIAA Paper 76-336, July 1976.

31) Dolling, D. S., C. D. Cosad and S. M. Bogdonoff, "An Examination of Blunt-Fin Induced Shock Wave Turbulent Boundary Layer Interactions," AIAA Paper No. 79-0068, Jan. 1979.

32) Settles, G. S., J. J. Perkins and S. M. Bogdonoff, "Investigation of Three-Dimensional Shock/Boundary-Layer Interactions at Swept Compression Corners," AIAA Journal, Vol. 18, July 1980, pp. 779-785.

33) Dolling, D. S. and S. M. Bogdonoff, "Upstream Influence Scaling of Sharp Fin-Induced Shock Wave Turbulent Boundary Layer Interactions," AIAA Paper 81-0336, Jan. 1981.

34) Horstman, C. C., G. S. Settles, I. E. Vas, S. M. Bogdonoff and C. M. Hung, "Reynolds Number Effects on Shock-Wave Turbulent Boundary-Layer Interactions," AIAA Journal, Vol. 15, Aug. 1977, pp. 1152-1158.

35) Settles, G. S., D. R. Williams, B. K. Baca and S. M. Bogdonoff, "Reattachment of a Compressible Turbulent Free Shear Layer," to appear shortly in AIAA Journal.

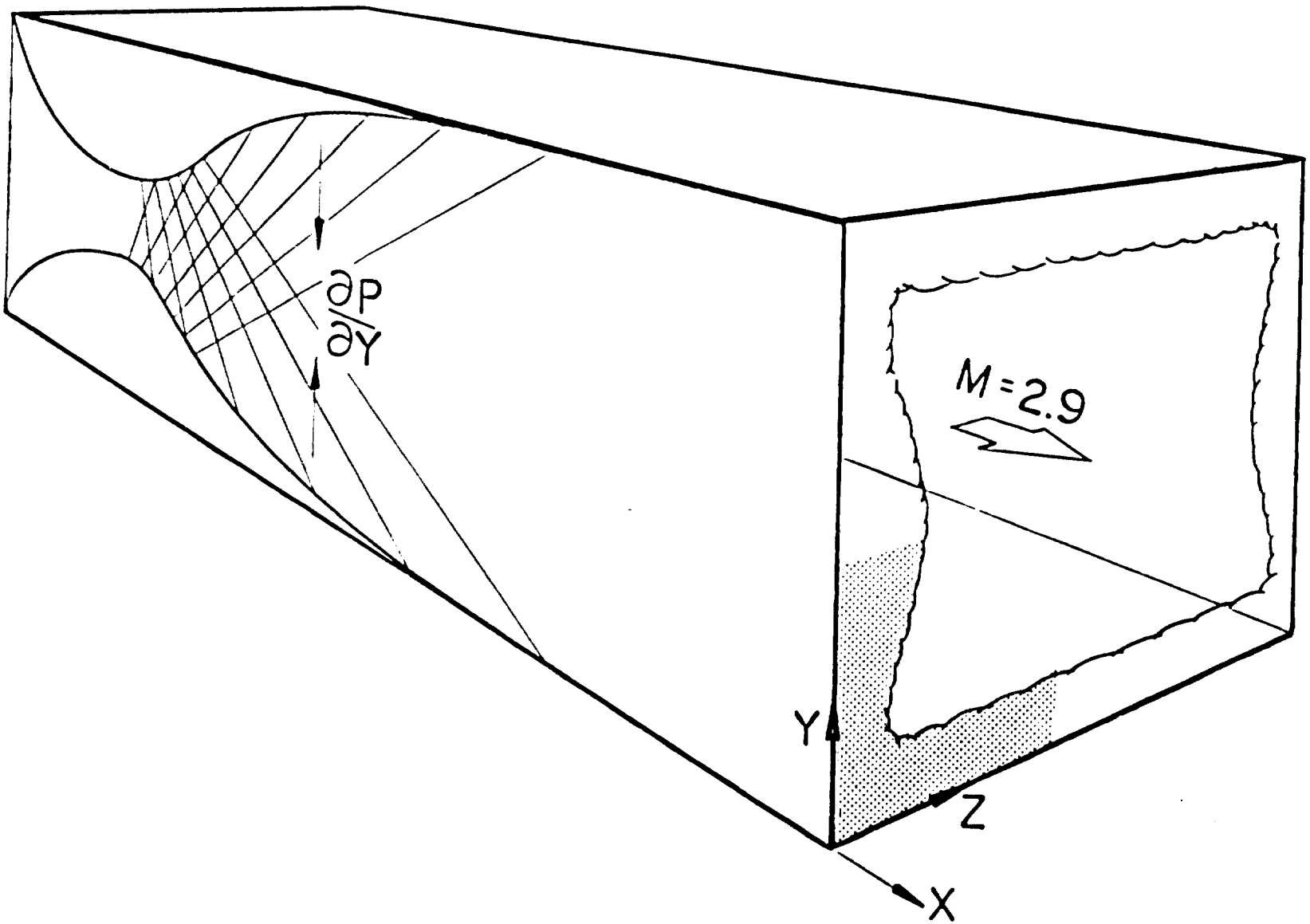

FIGURE 1. Flowfield Schematic of the Unbounded Streamwise Corner Flow.

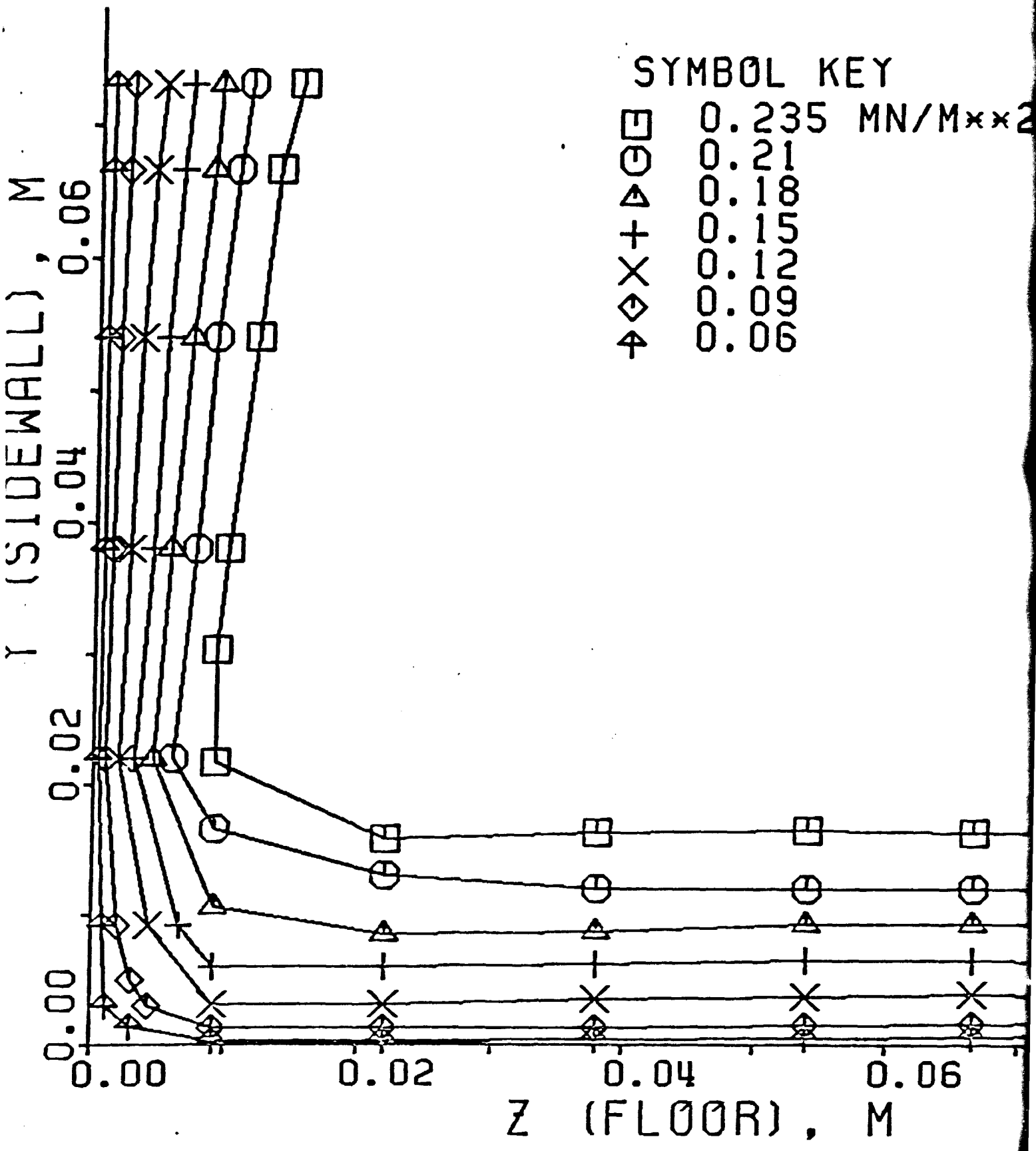

FIGURE 2. Corner Pitot Pressure Isobars in Tunnel Section 1.

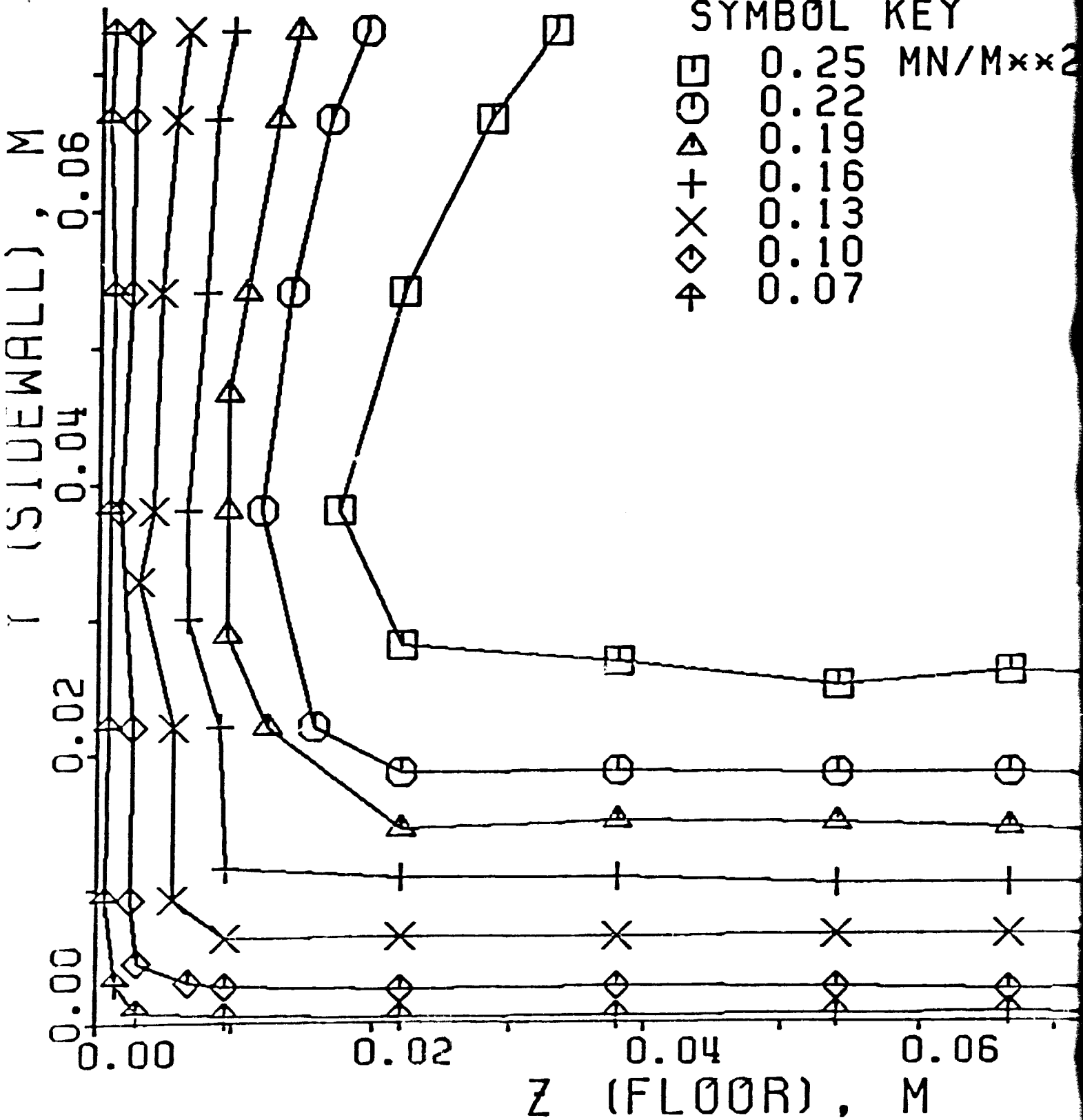

FIGURE 3. Corner Pitot Pressure Isobars in Tunnel Section 2.

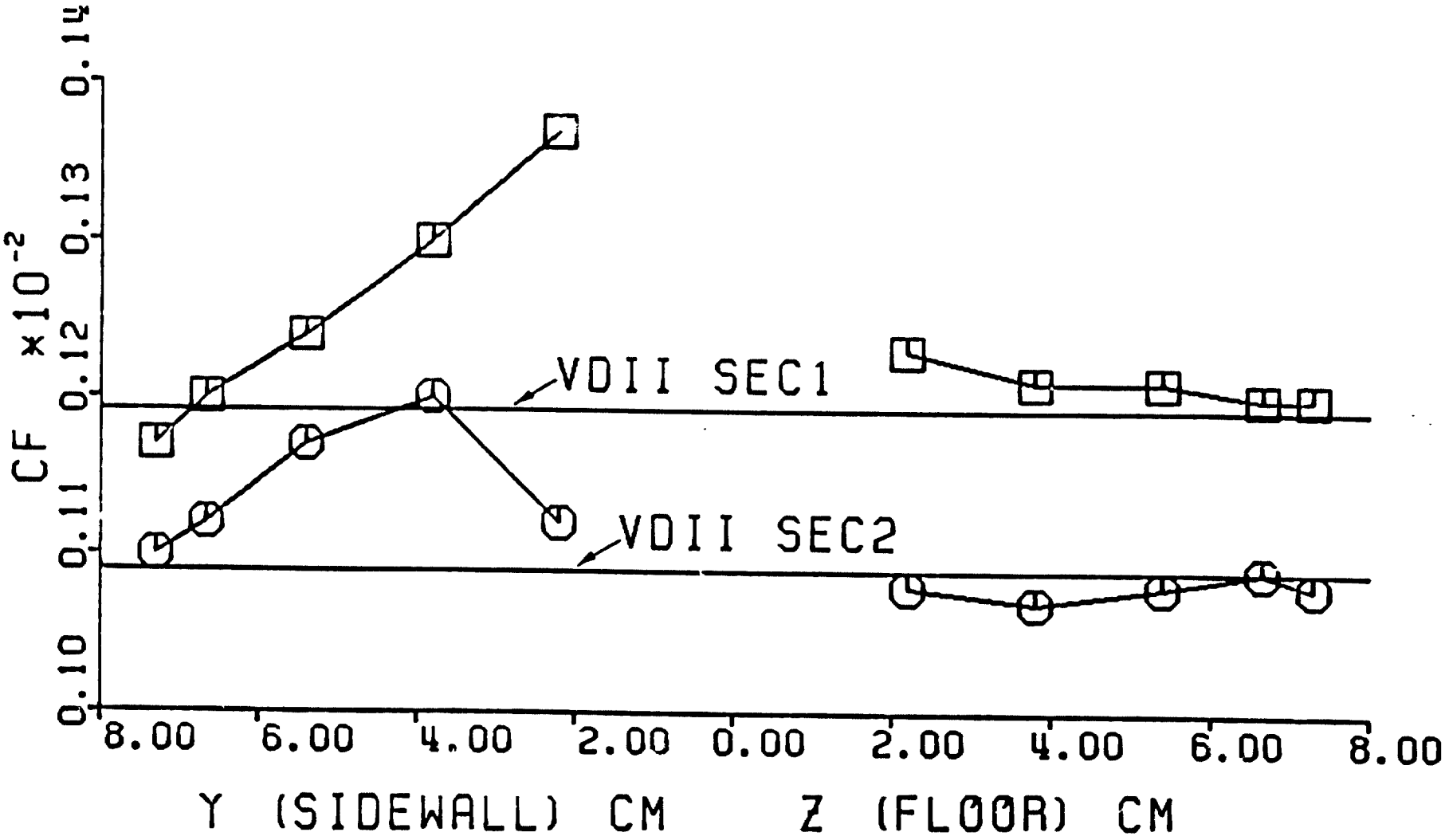

FIGURE 4. Streamwise Corner Skin Friction Distributions.

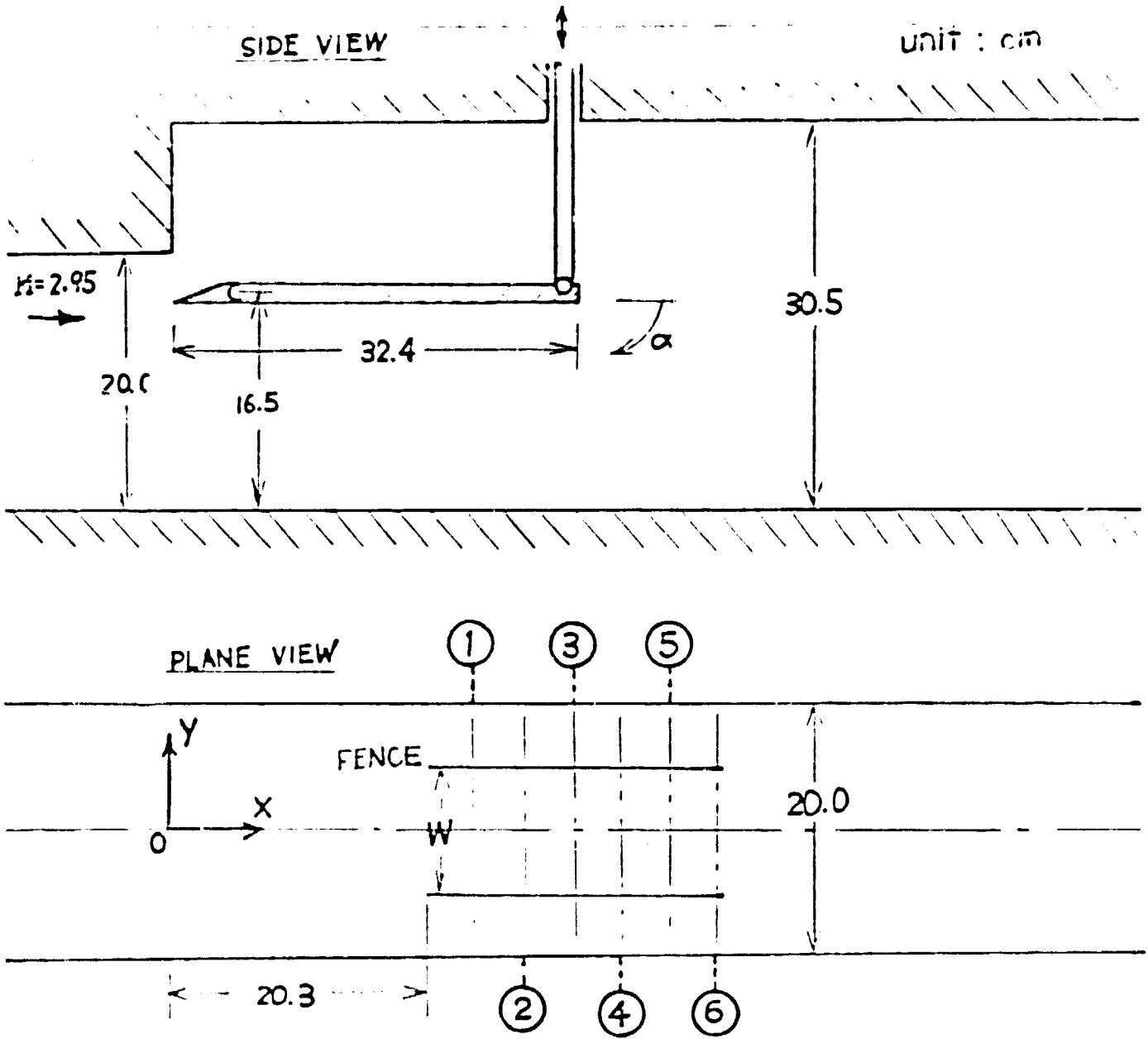

LOCATION OF CROSSWISE PRESSURE TAPS

Station No.	X (cm)
1	23.9
2	27.7
3	31.5
4	35.3
5	39.1
6	42.9

Fig. 5

unit : cm

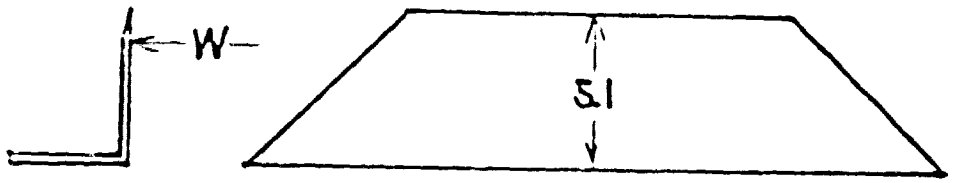

FENCE A

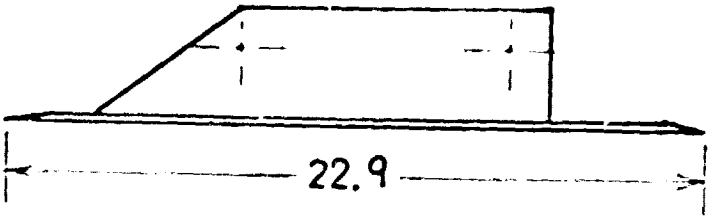

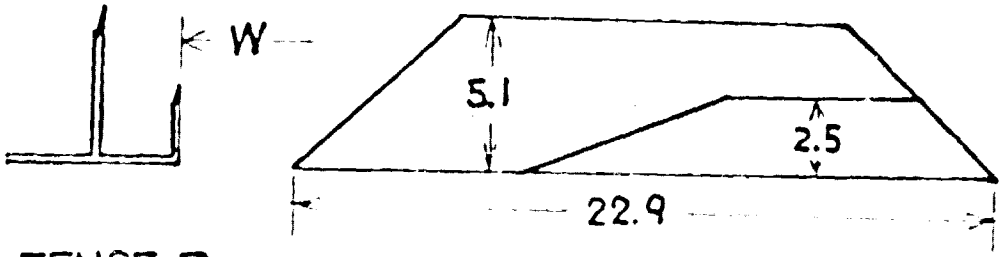

FENCE B

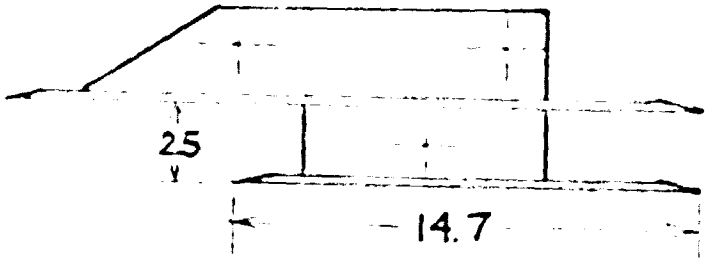

Case	Fence	W (cm)
I	A	12.7
II	A	8.9
III	B	8.9

Fig. 6

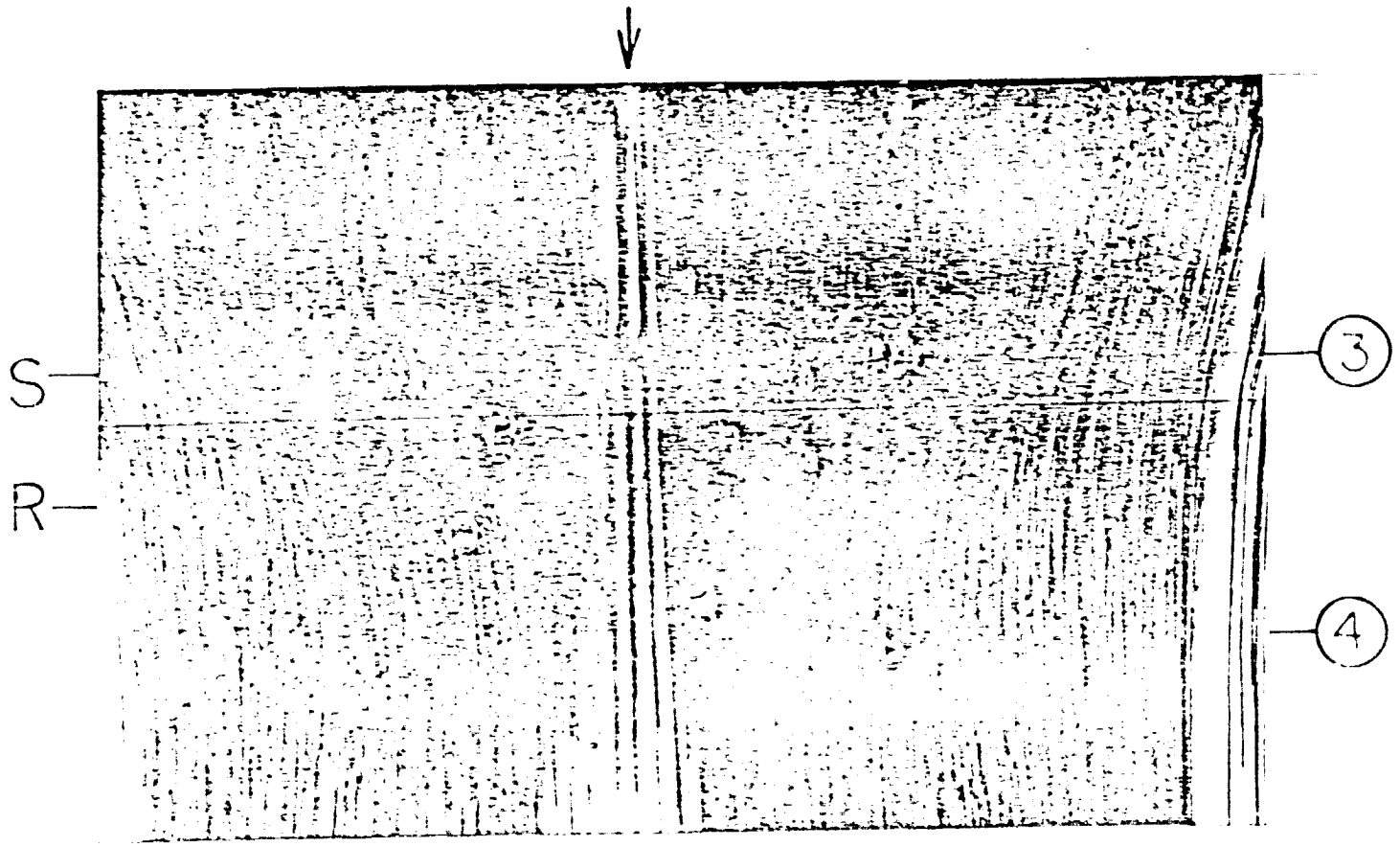

Fig. 7 Surface Flow Pattern $\alpha = 8^\circ$ Without Fences

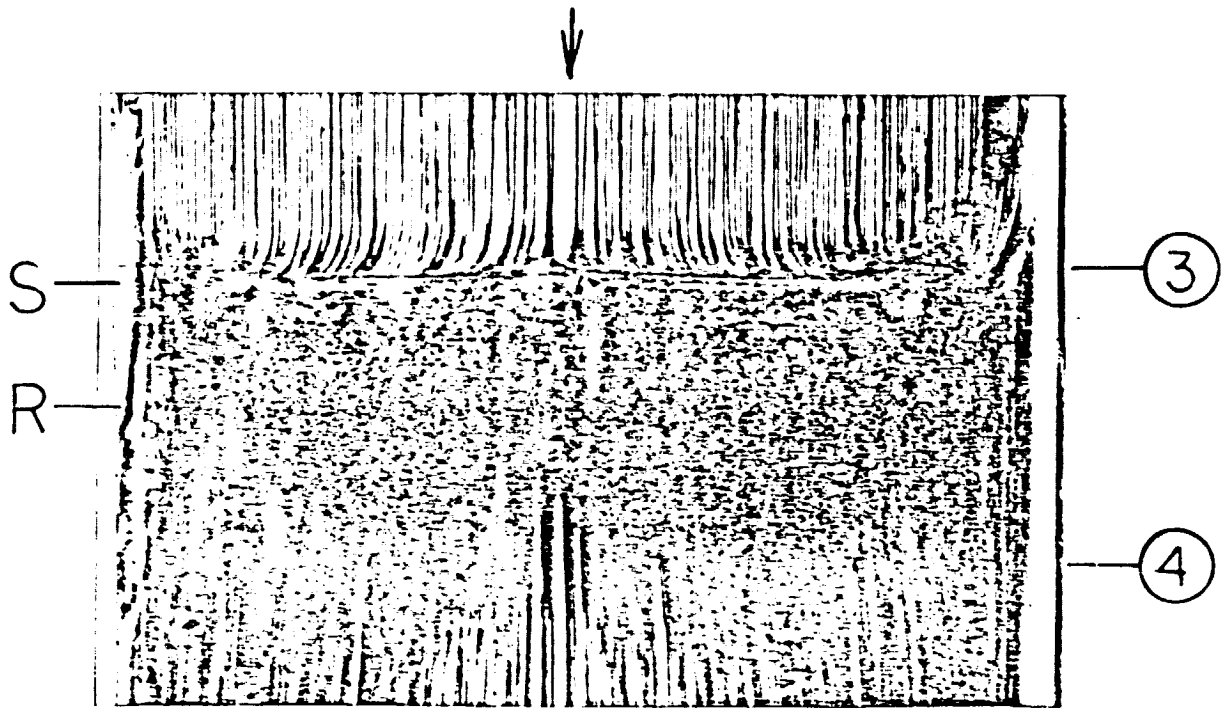

Fig. 8 Surface Flow Pattern $\alpha = 8°$ Case I

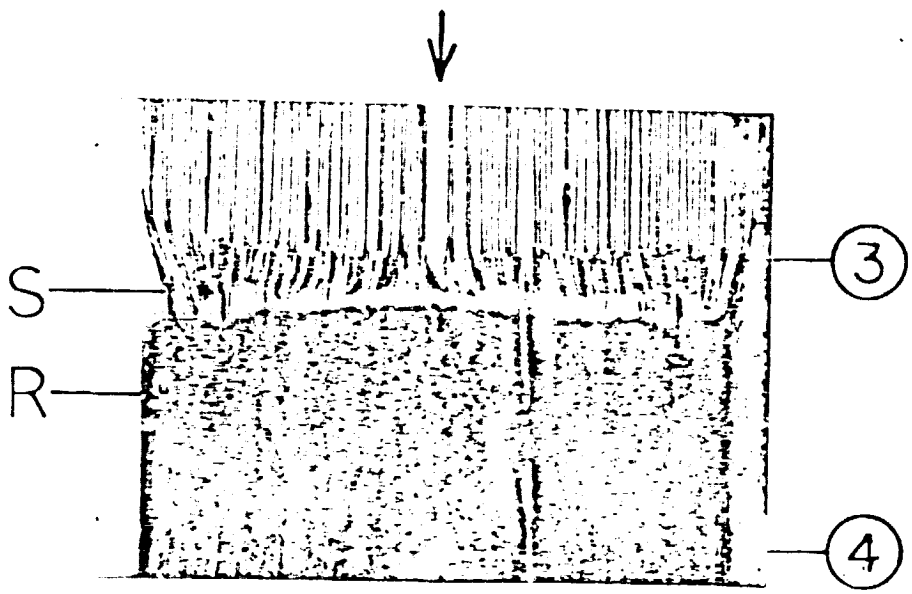

Fig. 9 Surface Flow Pattern $\alpha = 8°$ Case II

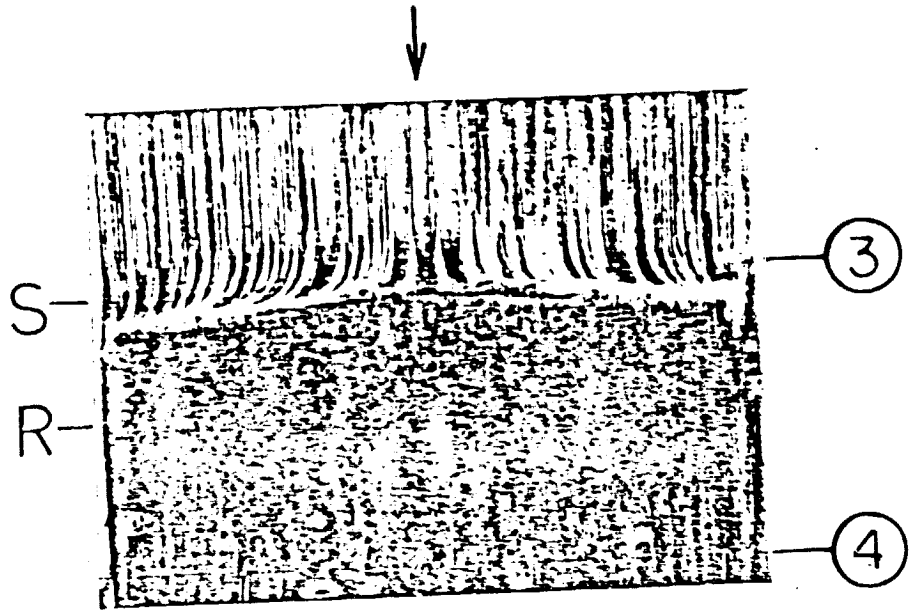

Fig. 10 Surface Flow Pattern $\alpha = 8^\circ$ Case III

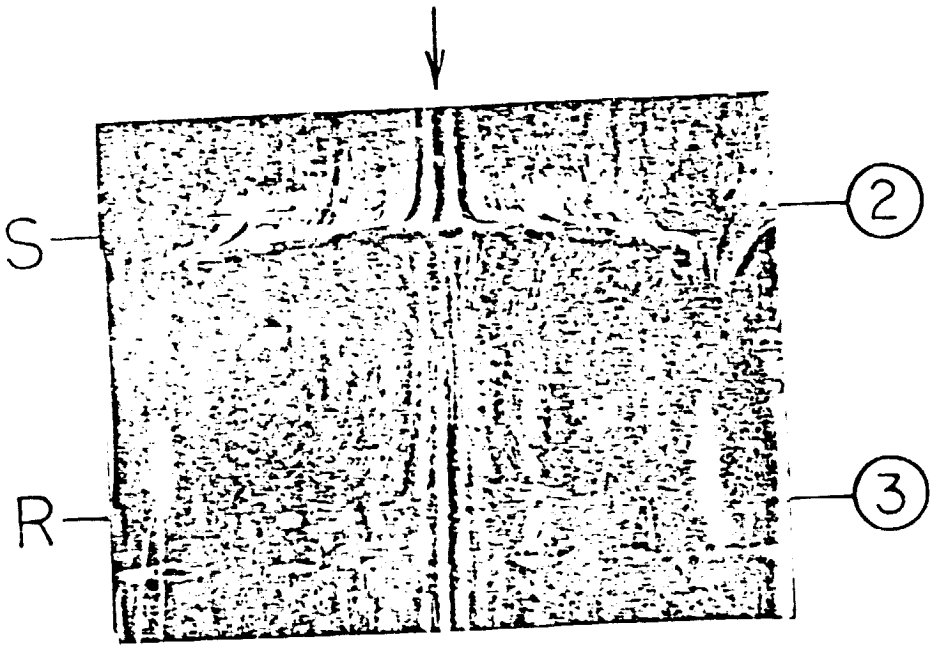

Fig. 11 Surface Flow Pattern $\alpha = 10^\circ$ Case III

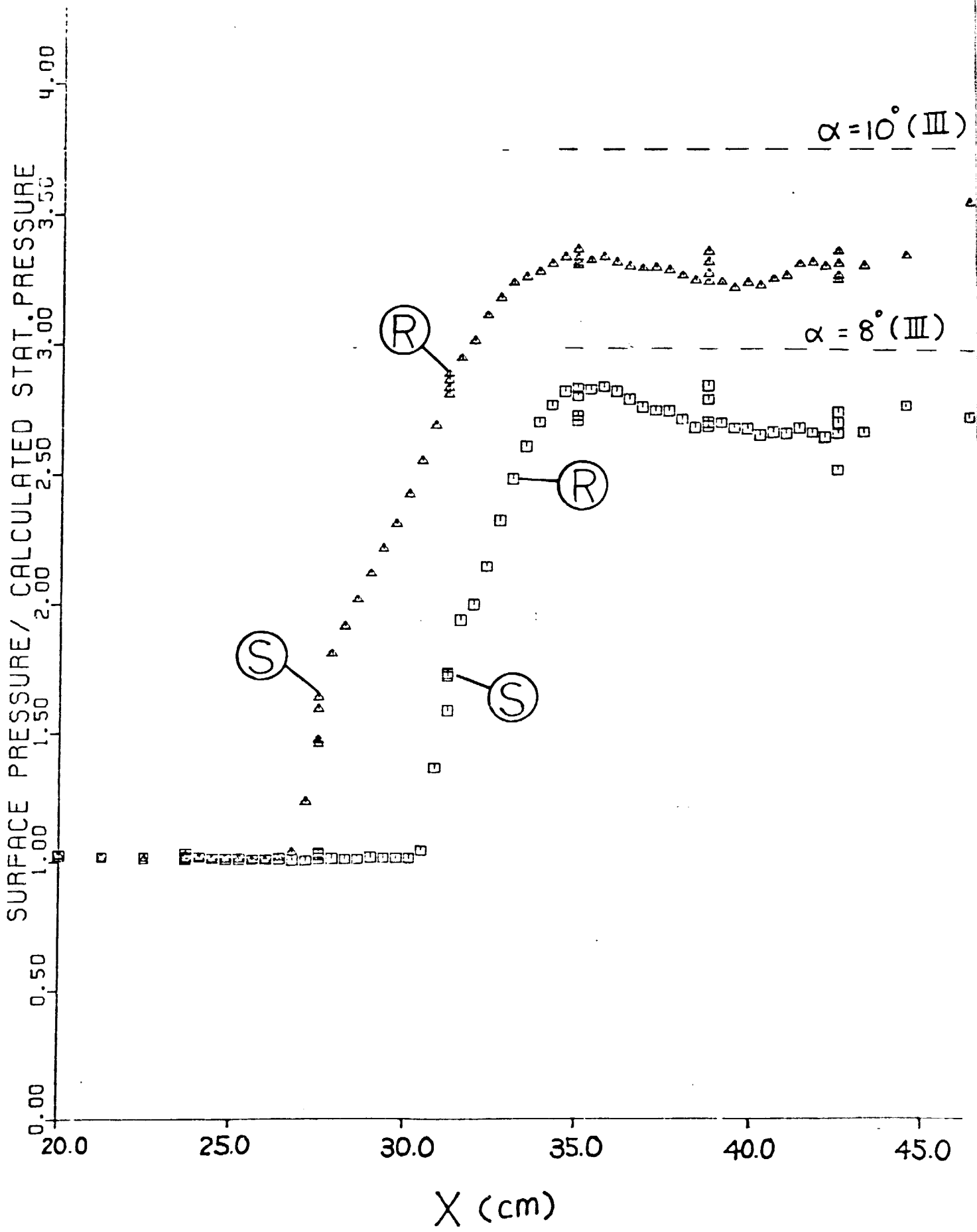

Fig. 12 Streamwise Surface Pressure Distributions

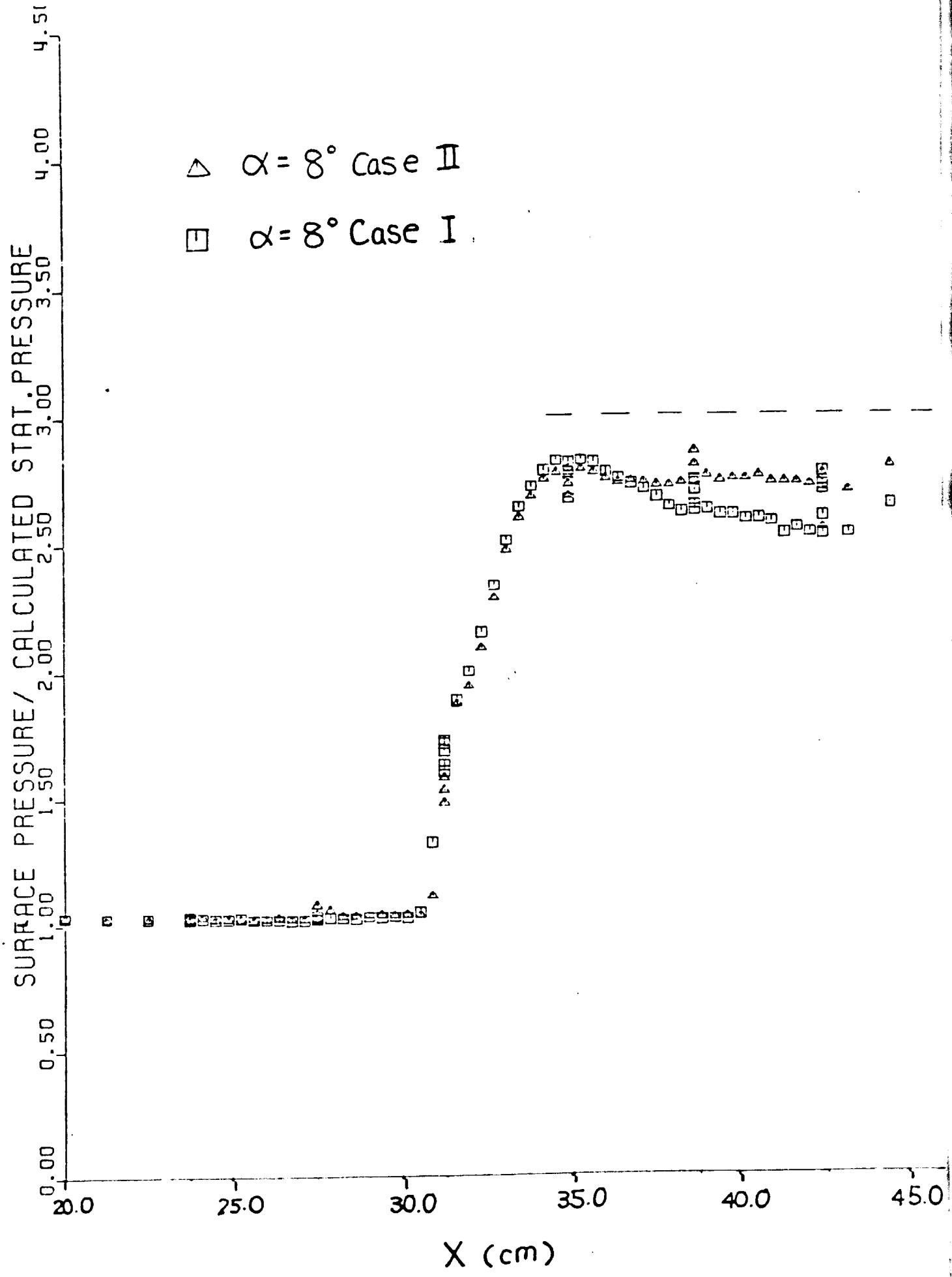

Fig. 13 Effect of Fence Distance on P-X Distribution

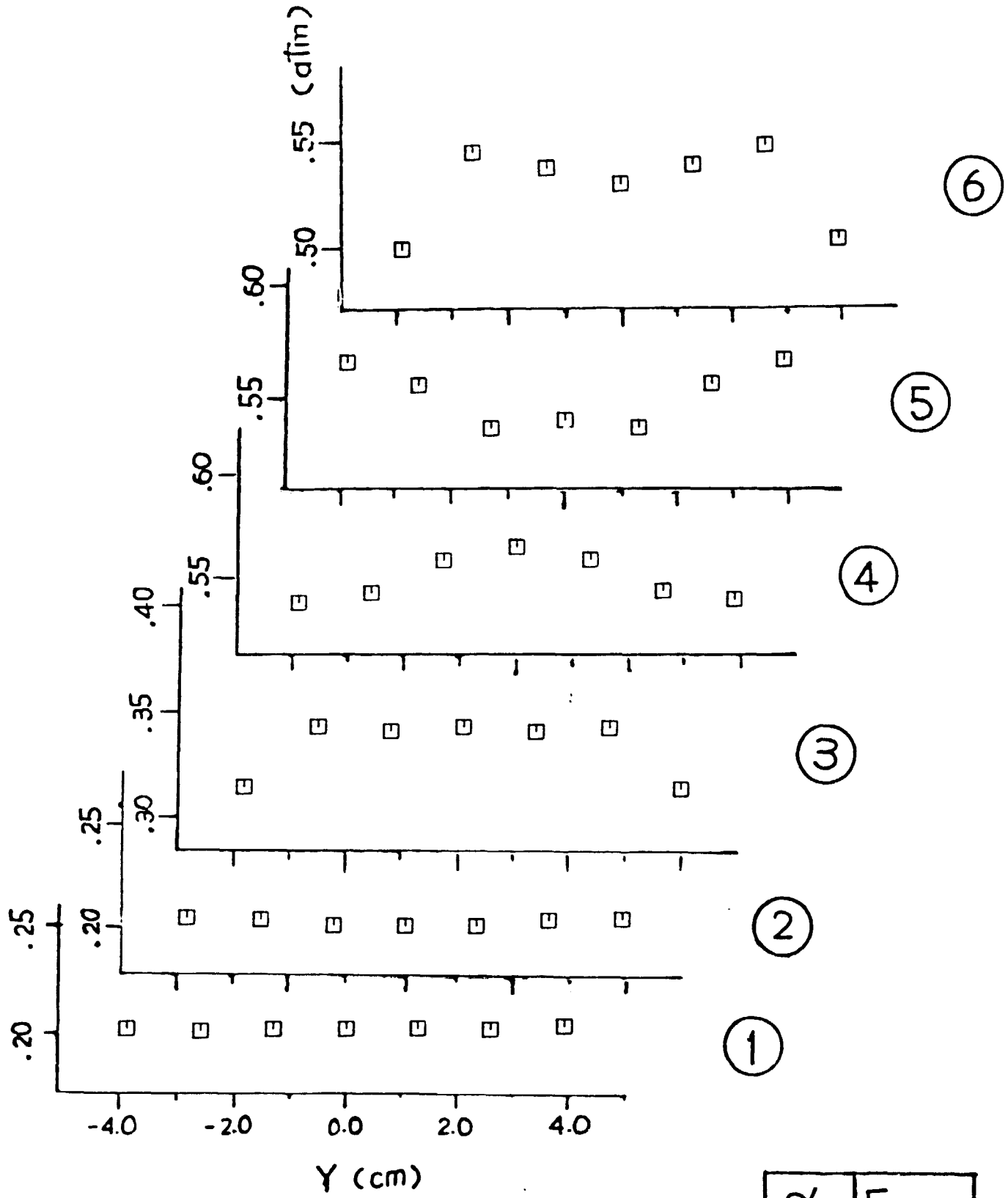

α	Fence
8°	III

Fig. 14 Crosswise Surface Pressure Distribution

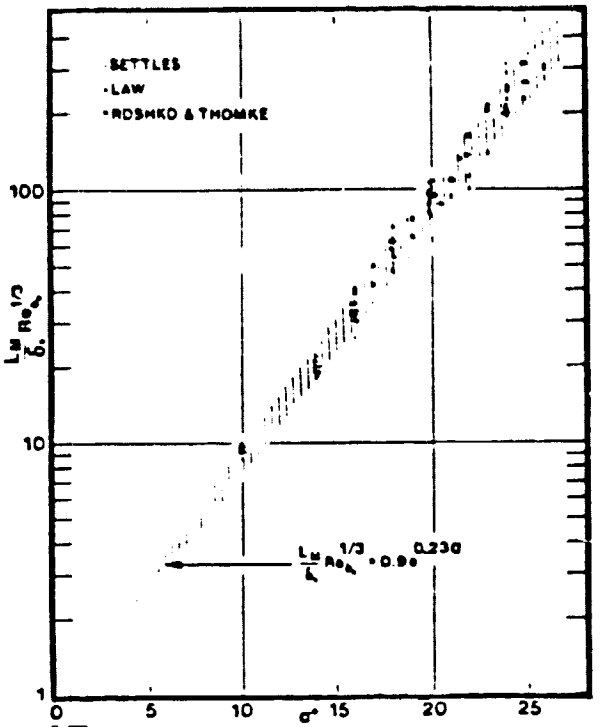

Fig. **15** Compression Corner Upstream Influence Correlation, M∞3, $10^5 \leq Re_{\delta_o} \leq 10^7$, $10^o \leq \alpha \leq 26^o$.

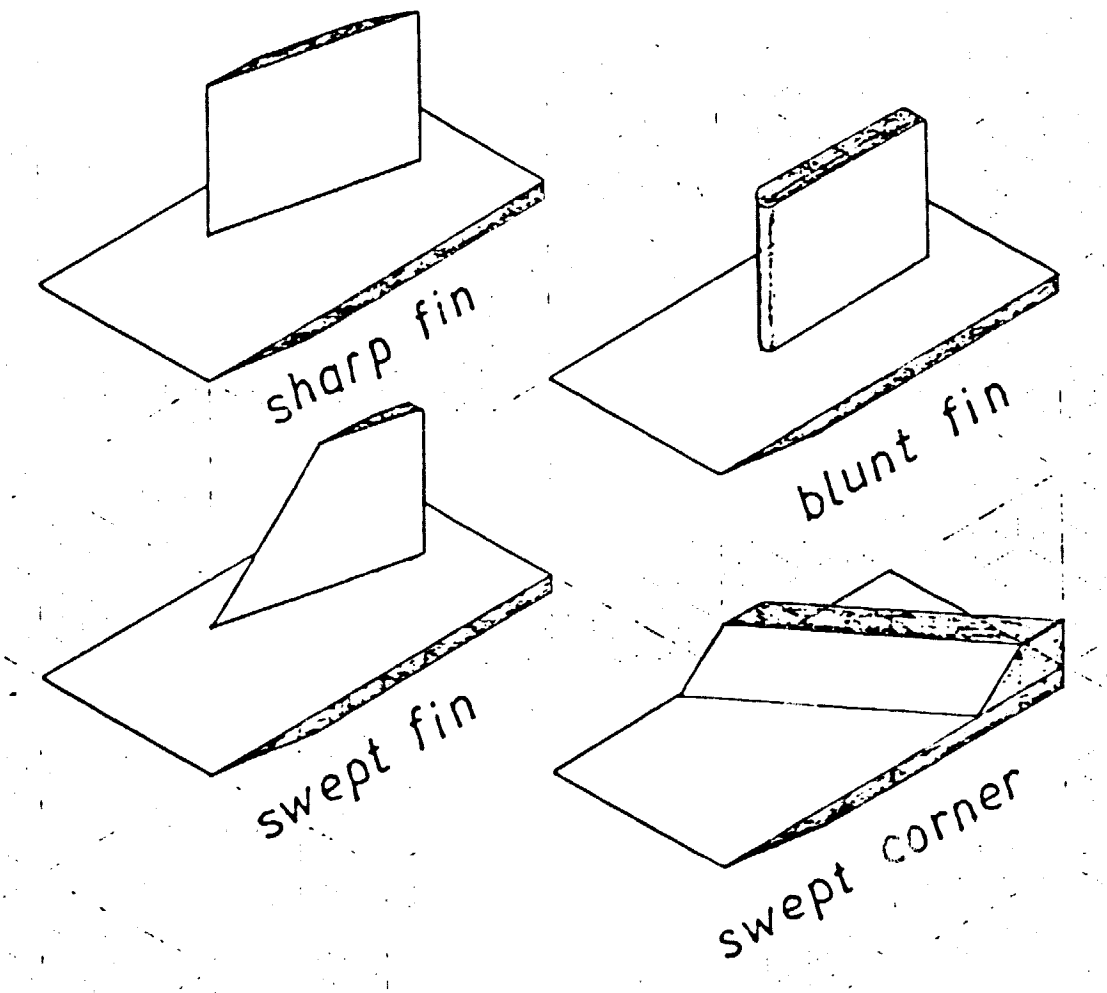

Fig. **16** Test Geometries for a Class of 3D Shock/Turbulent Boundary Layer Interactions.

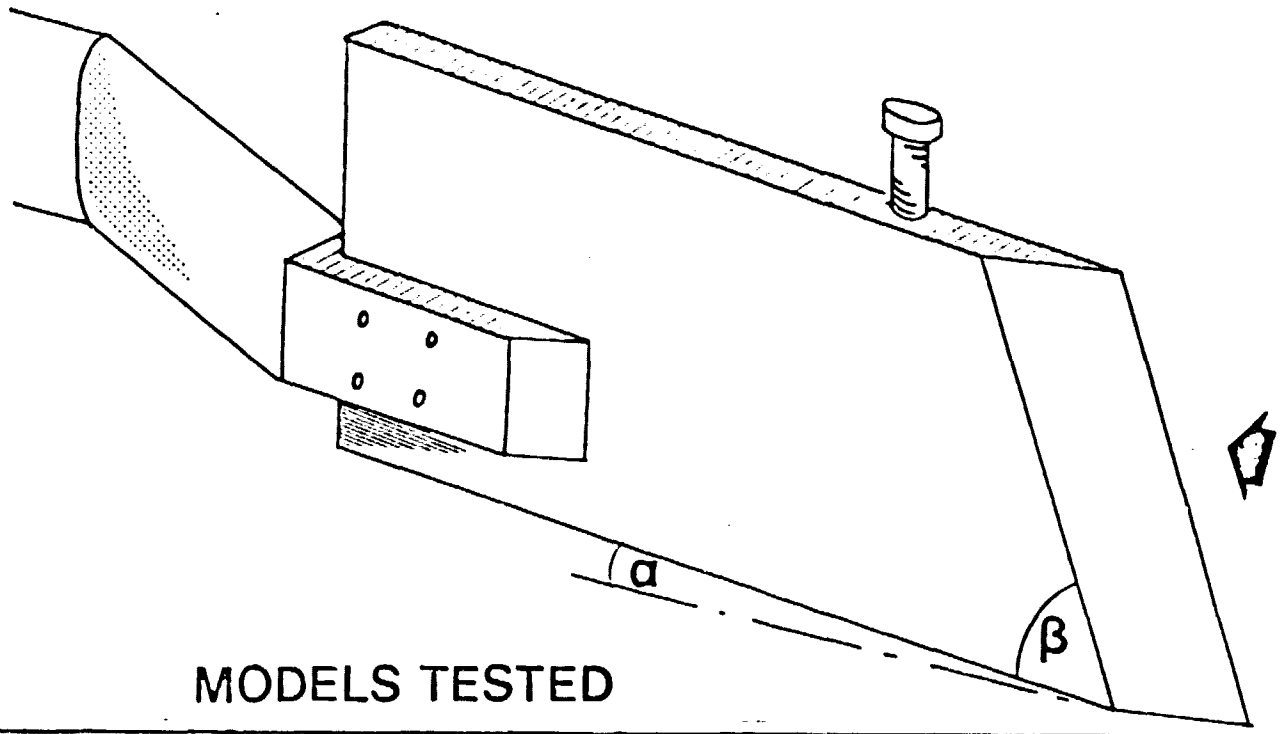

MODELS TESTED

α \ β	SYMBOL							
	90°	80°	70°	60°	50°	40°	35°	25°
5°	v	∧	N	◀	◁	▷	▷	◐
9°	×	+	⅄	Y	Z	✳	<	>
15°	o	○	◘	□	◆	◇	▲	△

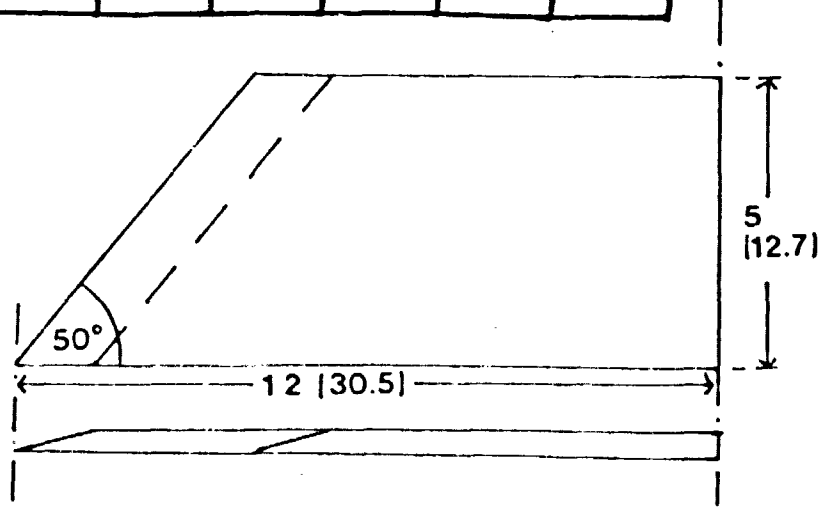

Fig. **17** Sketch of Swept Fin Geometry and Range of Parameters Tested.

Fig.18

THE KEROSENE-GRAPHITE SURFACE FLOW PATTERN FOR THE $\alpha = 9°$, $\beta = 35°$ FIN

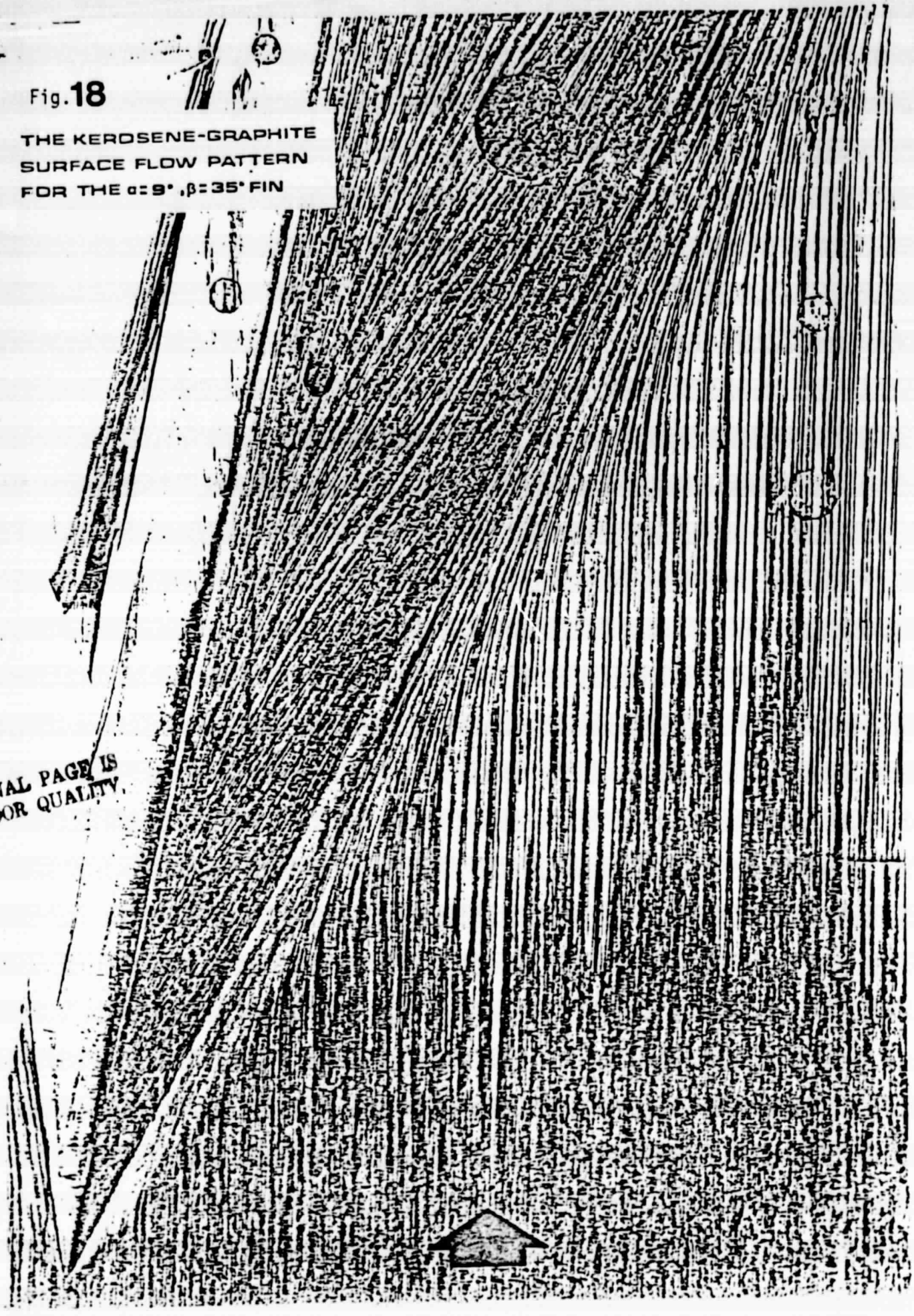

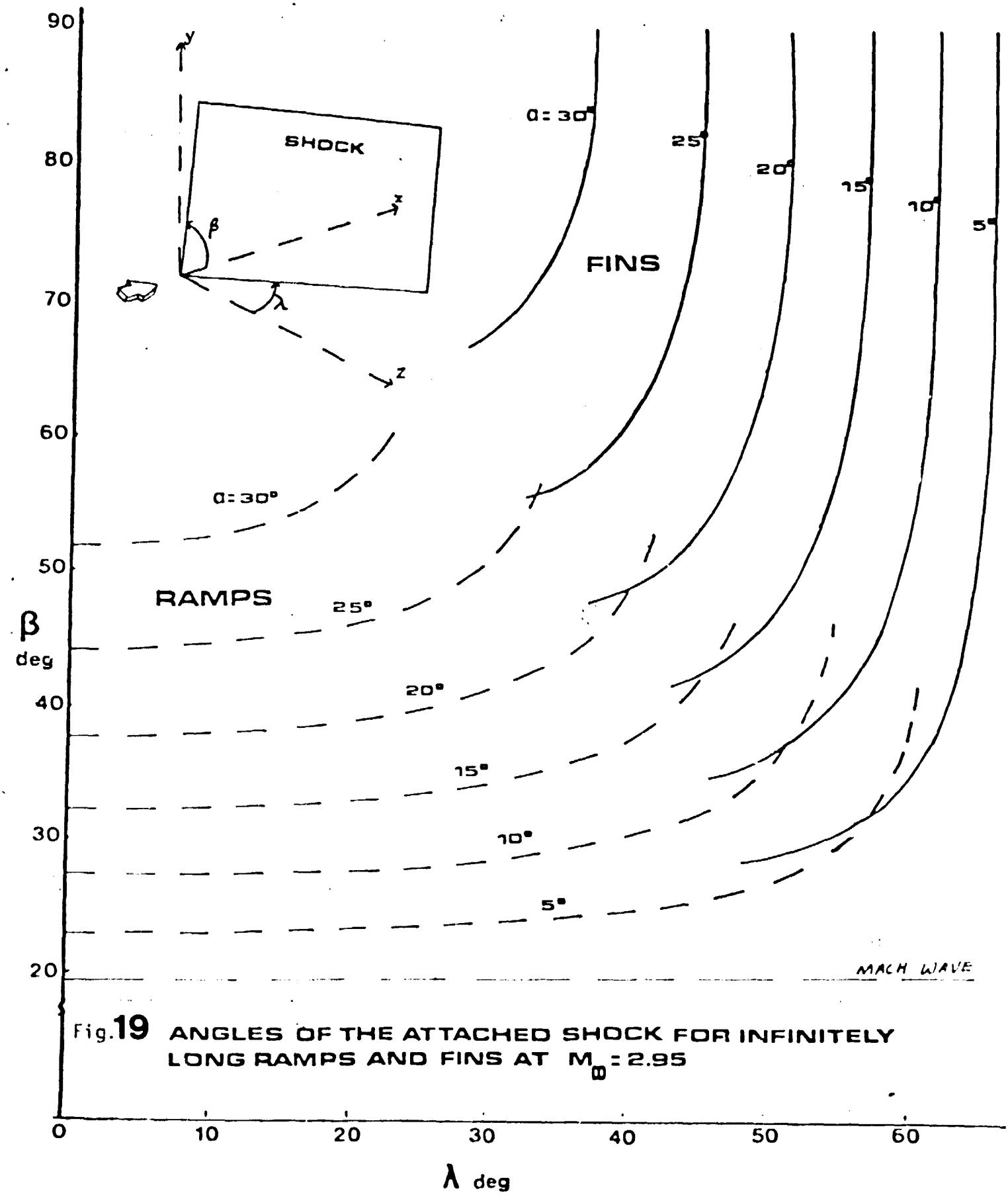

Fig. **19** ANGLES OF THE ATTACHED SHOCK FOR INFINITELY LONG RAMPS AND FINS AT $M_\infty = 2.95$